Electronic Supplementary Material (ESI) for Dalton Transactions.

Electronic Supplementary Information for:

Modulation of N^N'-bidentate chelating pyridyl-pyridylidene amide ligands offers mechanistic insights into Pd-catalysed ethylene/methyl acrylate copolymerisation

Gearóid M. Ó Máille,[a] *Anna Dall'Anese,*[b,c] *Philipp Grossenbacher,*[a] *Tiziano Montini,*[b] *Barbara Milani,*[b,*] *and Martin Albrecht.*[a,*]

[a]Department of Chemistry & Biochemistry, University of Bern, Freiestrasse 3, CH-3012 Bern, Switzerland
[b]Dipartimento di Scienze Chimiche e Farmaceutiche, Università di Trieste, Via Licio Giorgieri 1, 34127 Trieste, Italy
[c]Current address: Department of Chemistry, Biology and Biotechnology, University of Perugia, Via Elce di Sotto 8, 06123 - Perugia, Italy

E-mail: milaniba@units.it; martin.albrecht@dcb.unibe.ch

Table of contents

1. NMR spectra of all ligand precursors and complexes

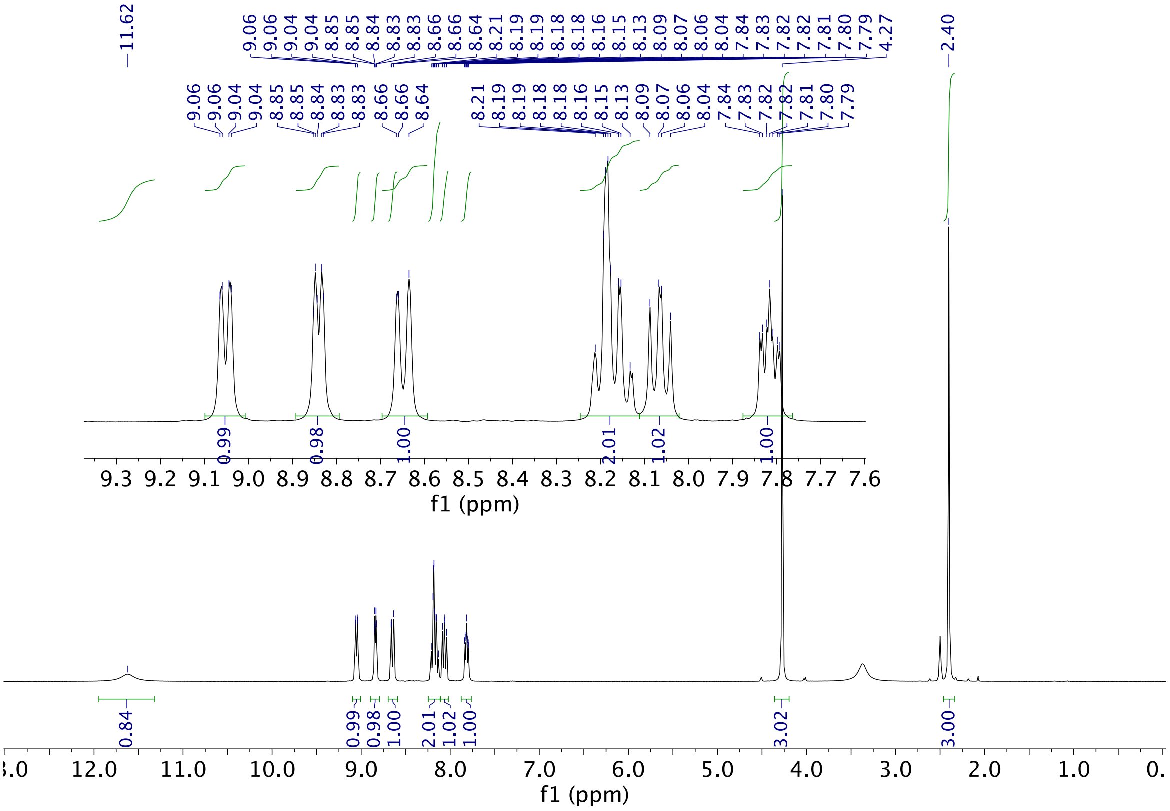

Figure S1. ^{1}H NMR spectrum (DMSO-d_6, 300 MHz) of pyridinium salt **6**.

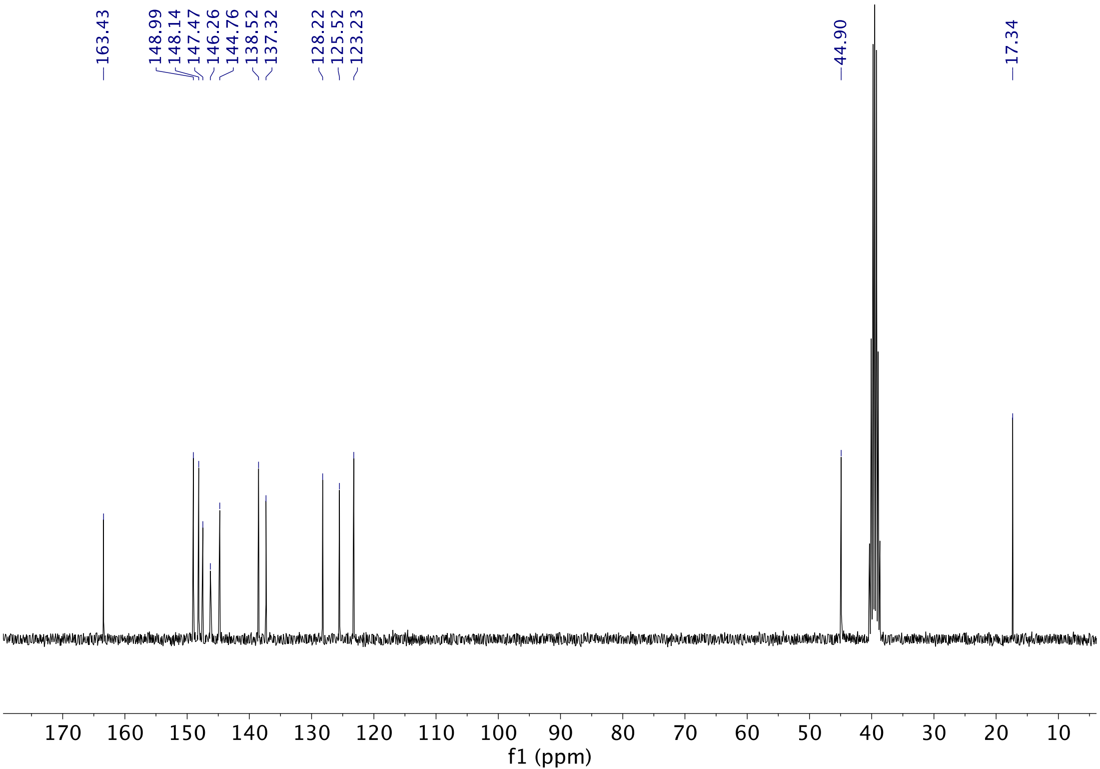

Figure S2^{13}C NMR spectrum (DMSO-d_6, 300 MHz) of pyridinium salt **6**.

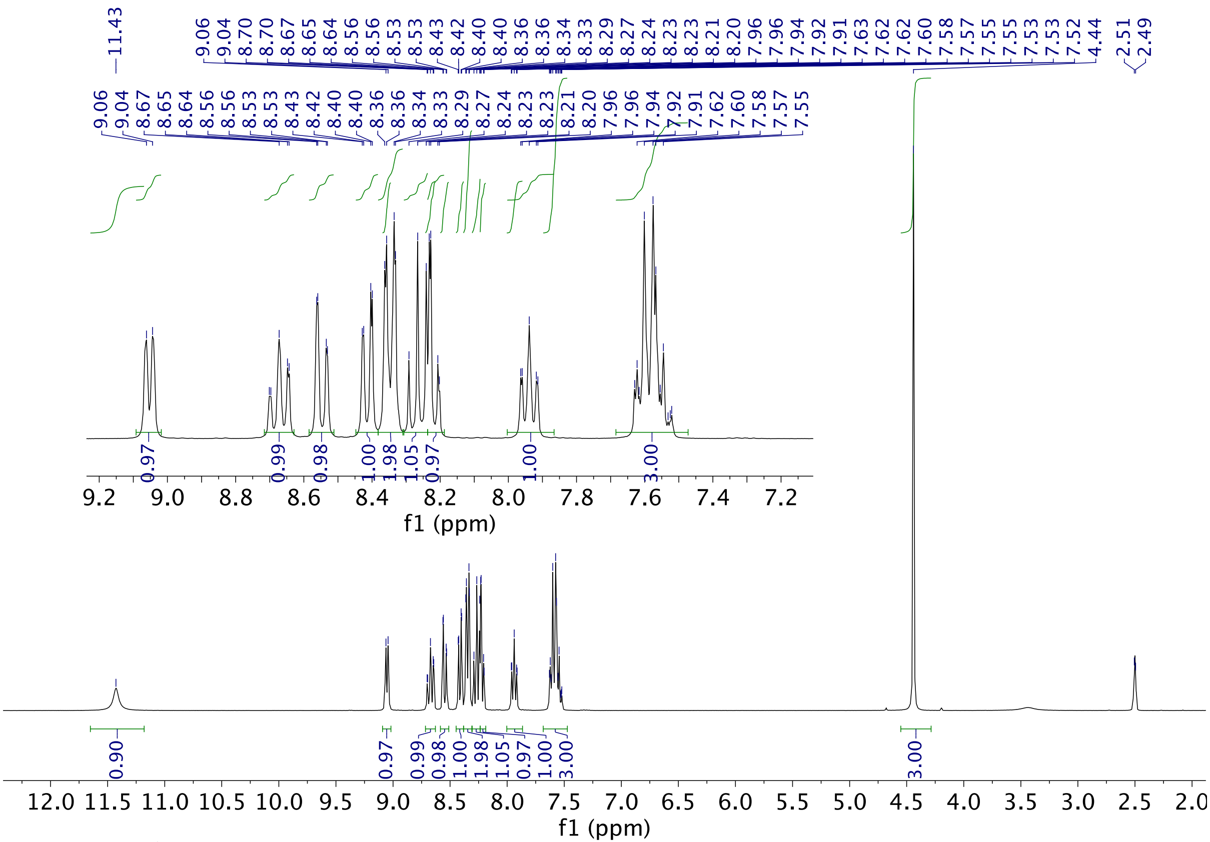

Figure S3. ^{1}H NMR spectrum (DMSO-d_6, 300 MHz) of pyridinium salt **7**.

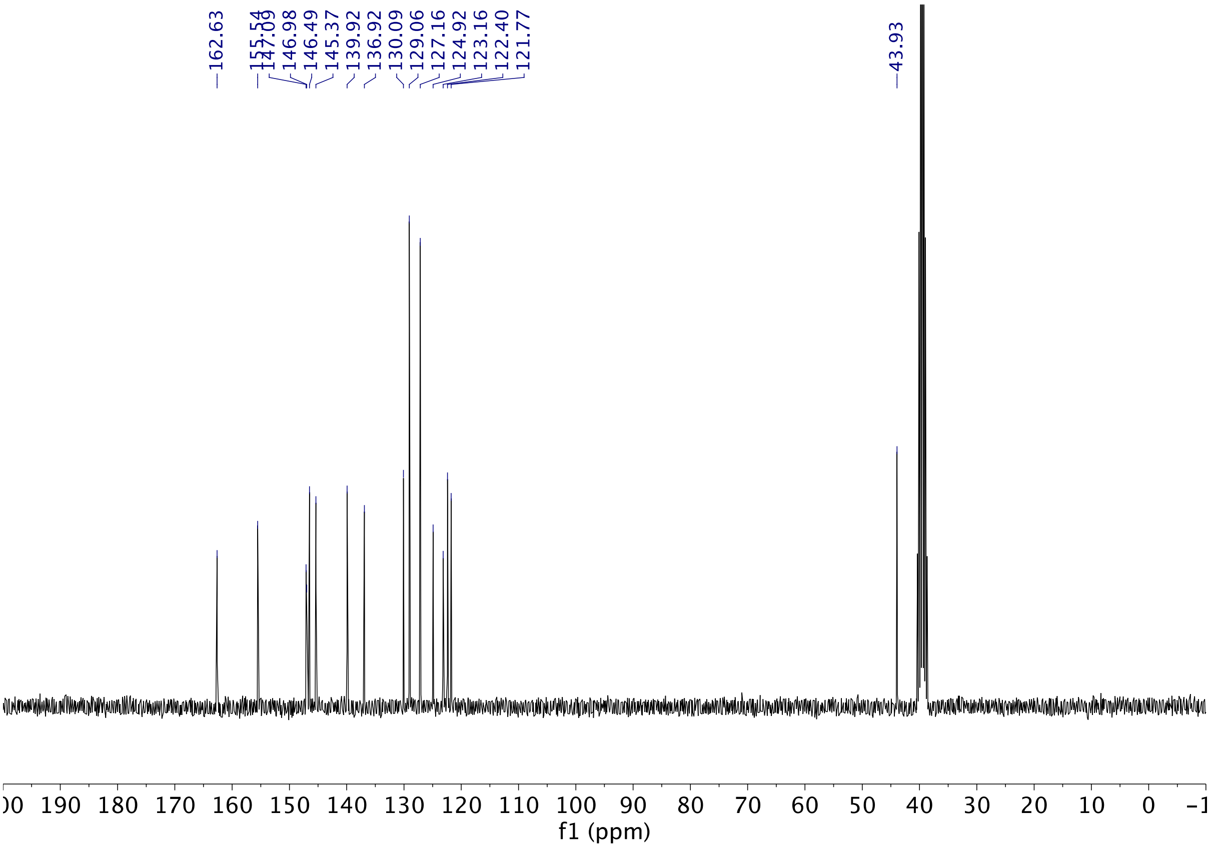

Figure S4. ^{13}C NMR spectrum (DMSO-d_6, 300 MHz) of pyridinium salt **7**.

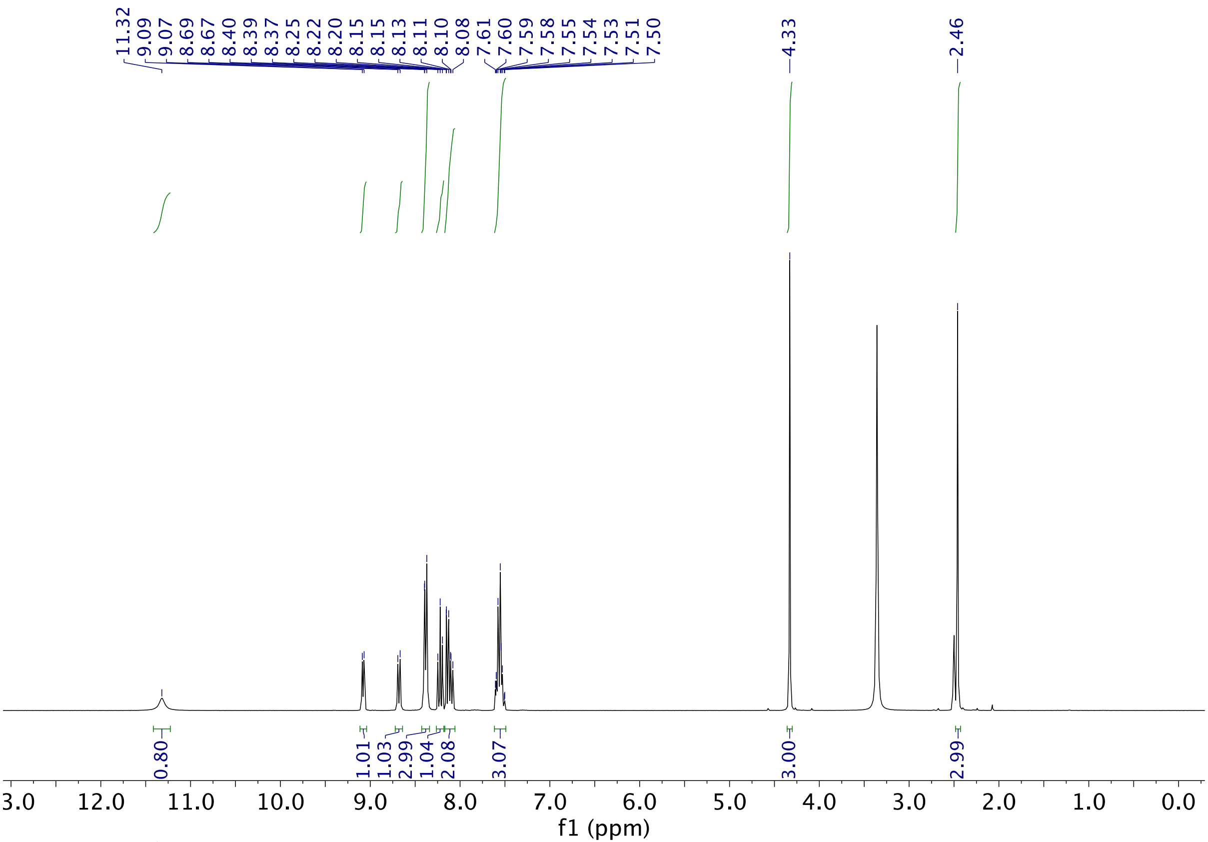

Figure S5. ^{1}H NMR spectrum (DMSO-d_6, 300 MHz) of pyridinium salt **8**.

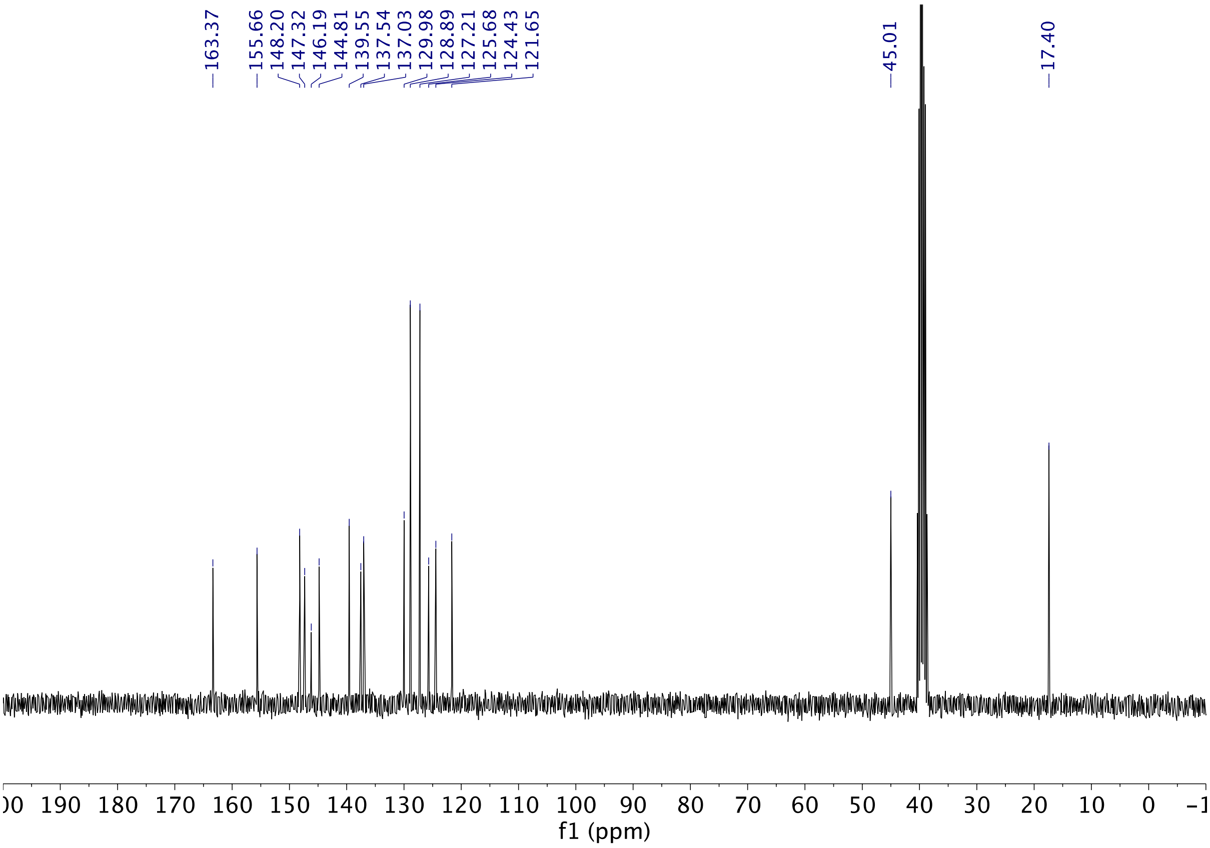

Figure S6. ^{13}C NMR spectrum (DMSO-d_6, 300 MHz) of pyridinium salt **8**.

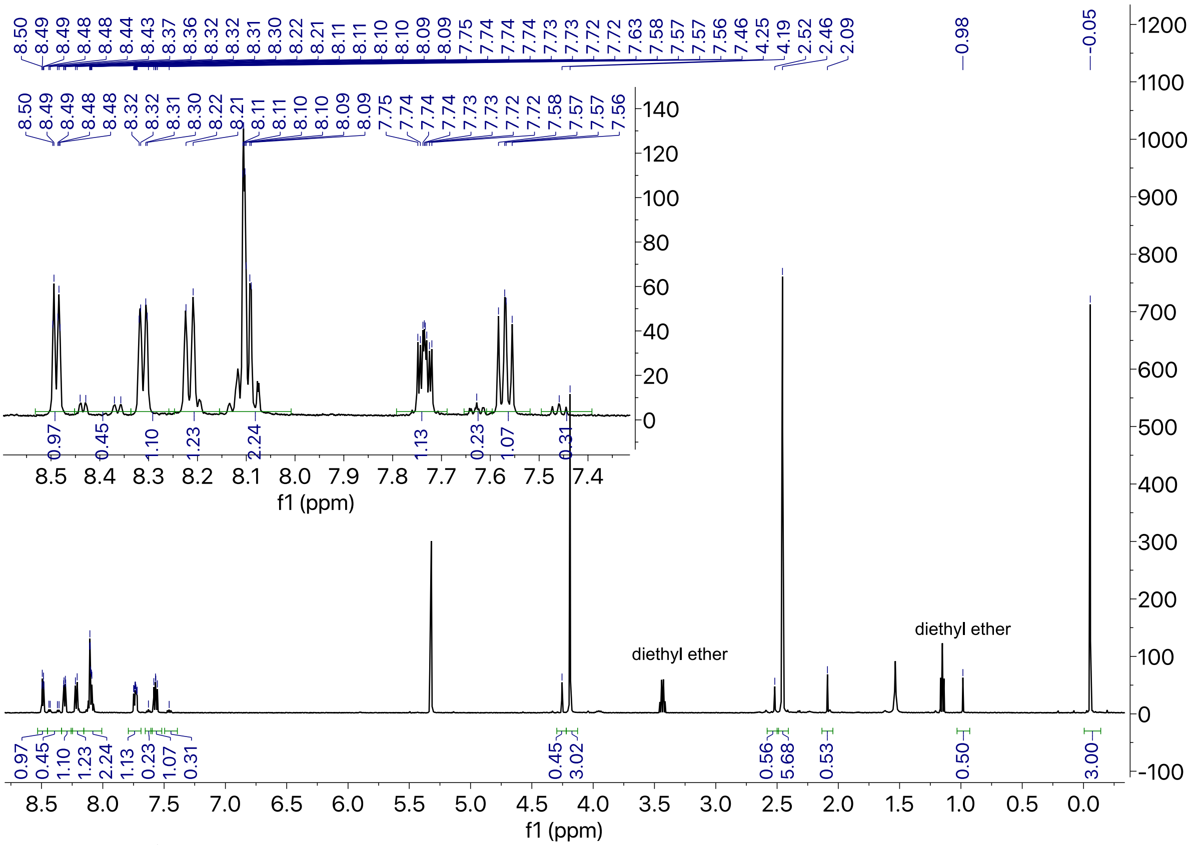

Figure S7. ^{1}H NMR spectrum (CD_2Cl_2, 300 MHz) of complex **10**.

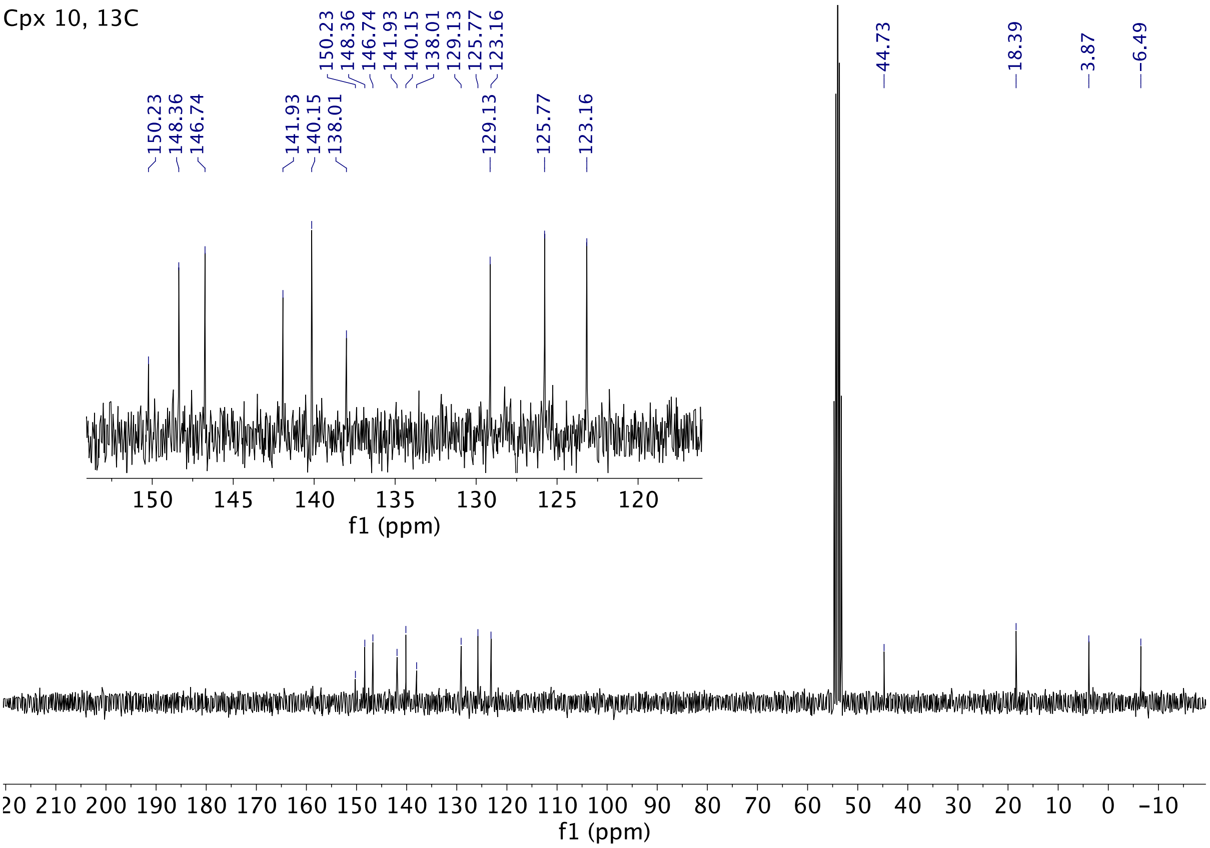

Figure S8. ^{13}C NMR spectrum (CD_2Cl_2, 300 MHz) of complex **10**.

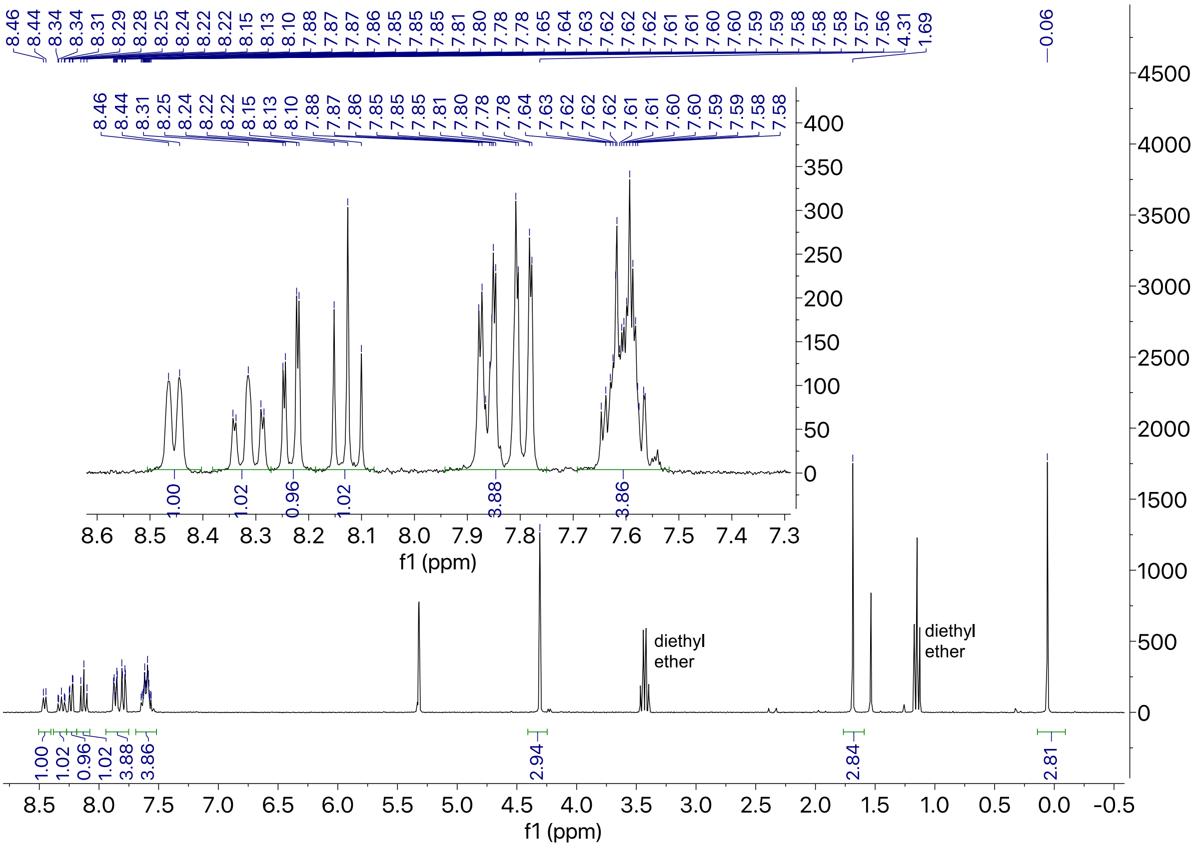

Figure S9. ^{1}H NMR spectrum (CD_2Cl_2, 300 MHz) of complex **11**.

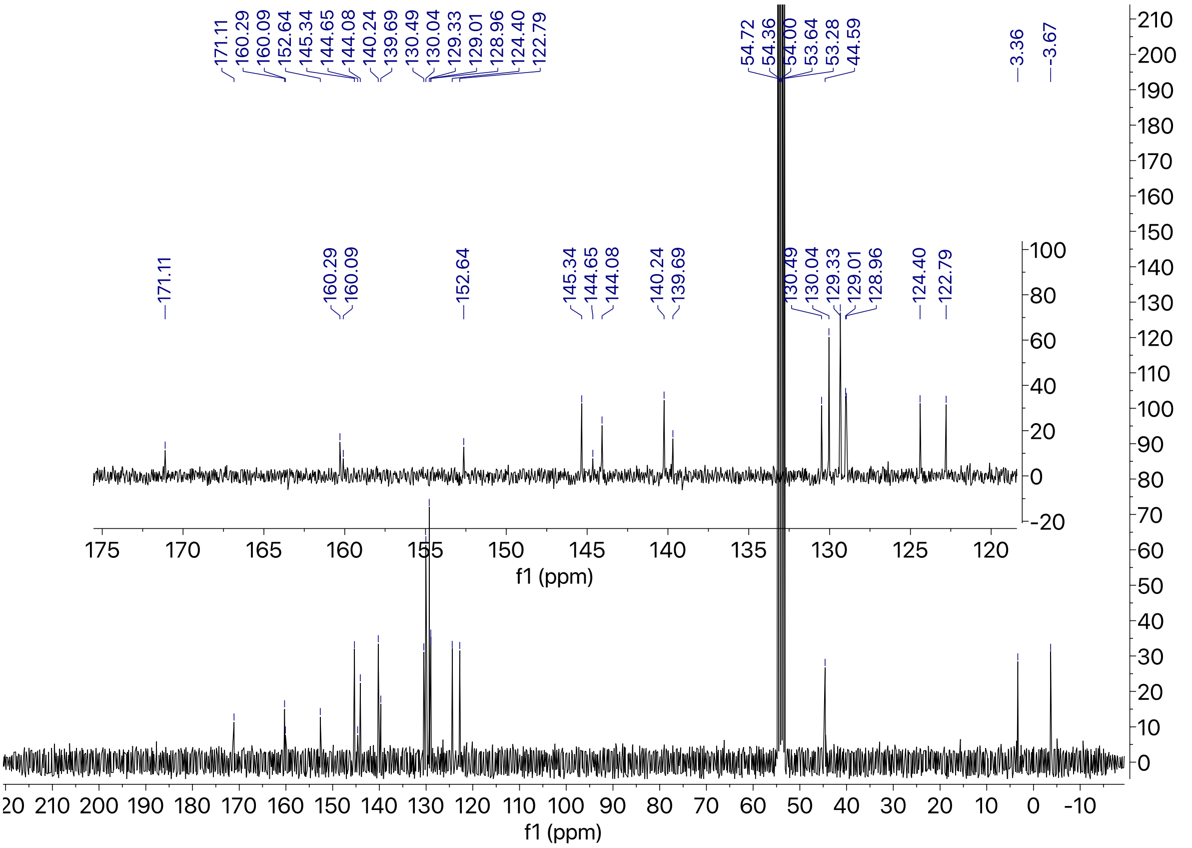

Figure S10. ^{13}C NMR spectrum (CD_2Cl_2, 300 MHz) of complex **11**.

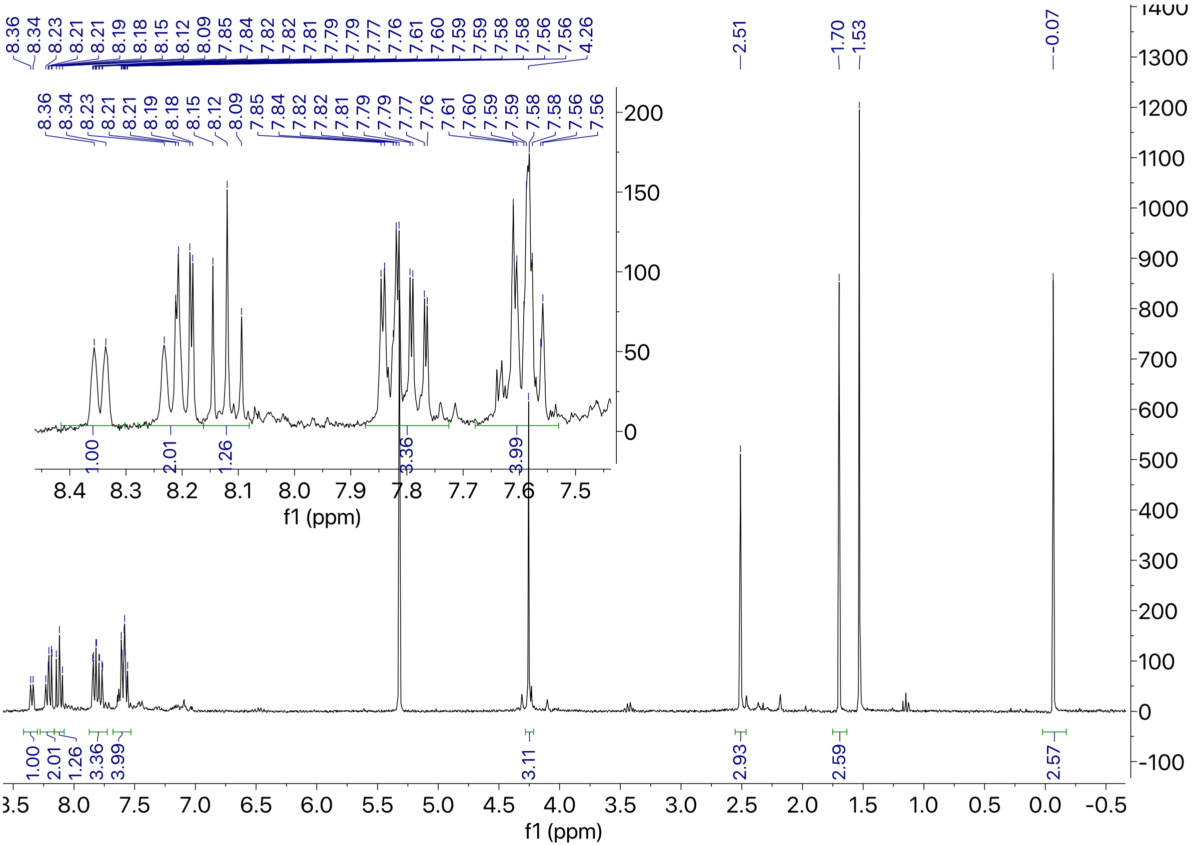

Figure S11. ^{1}H NMR spectrum (CD_2Cl_2, 300 MHz) of complex **12**.

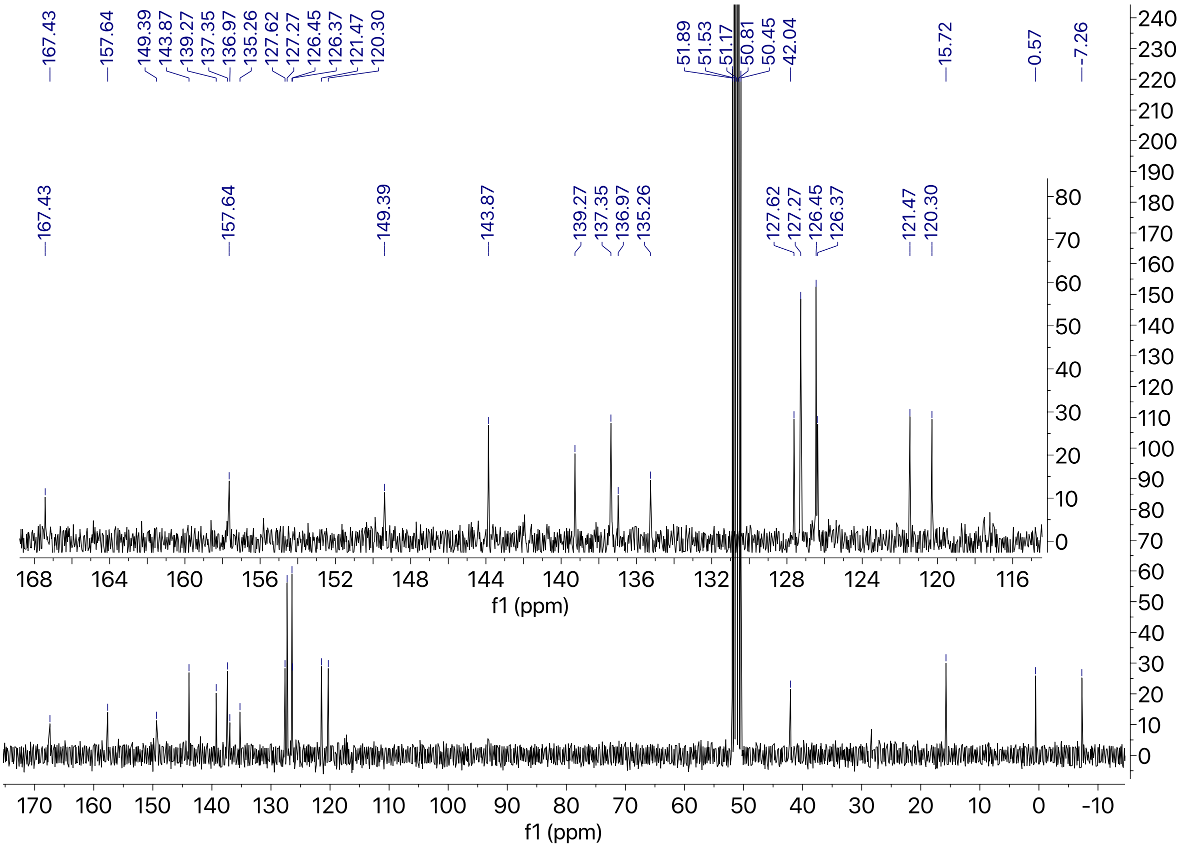

Figure S12. ^{13}C NMR spectrum (CD_2Cl_2, 300 MHz) of complex **12**.

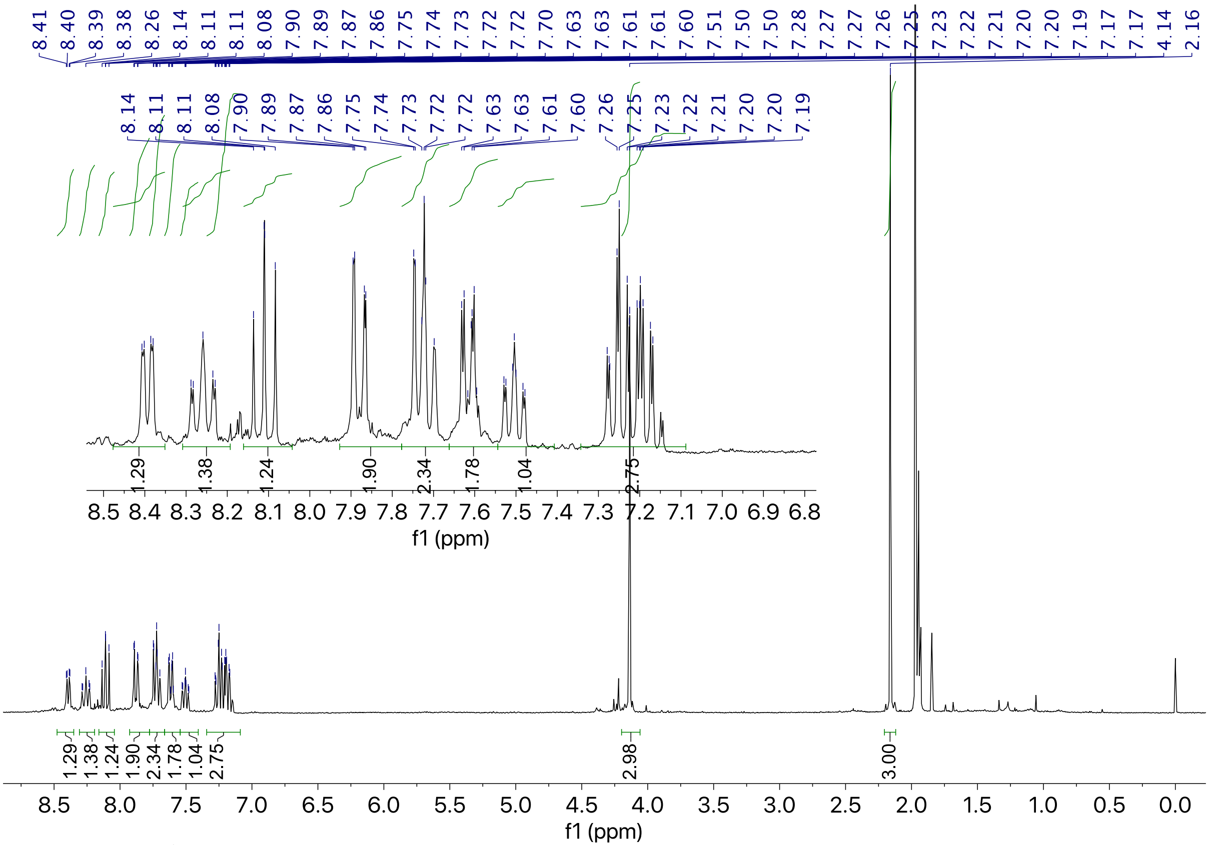

Figure S13. ^{1}H NMR spectrum (CD$_3$CN, 300 MHz) of complex **13**.

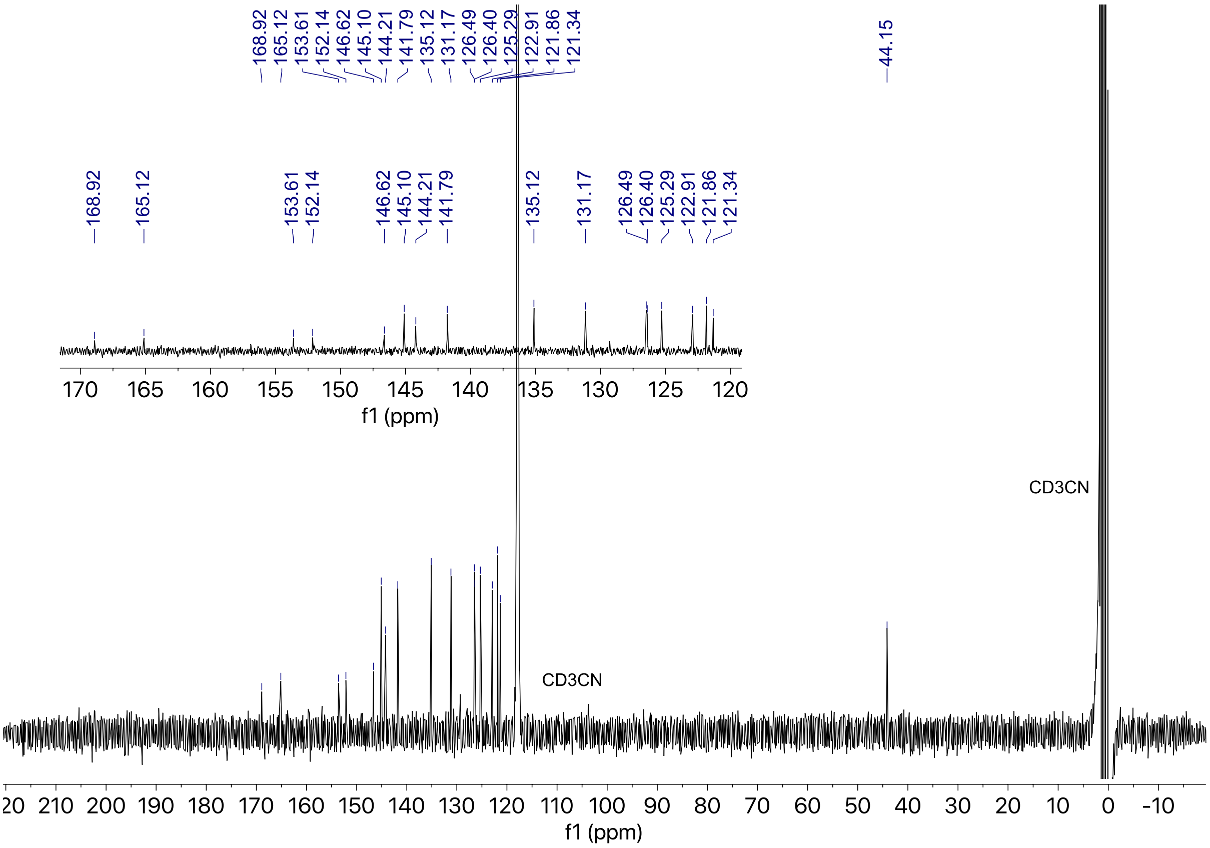

Figure S14. ^{13}C NMR spectrum (CD$_3$CN, 300 MHz) of complex **13**.

2. NMR spectroscopic analysis of catalytic products and intermediates

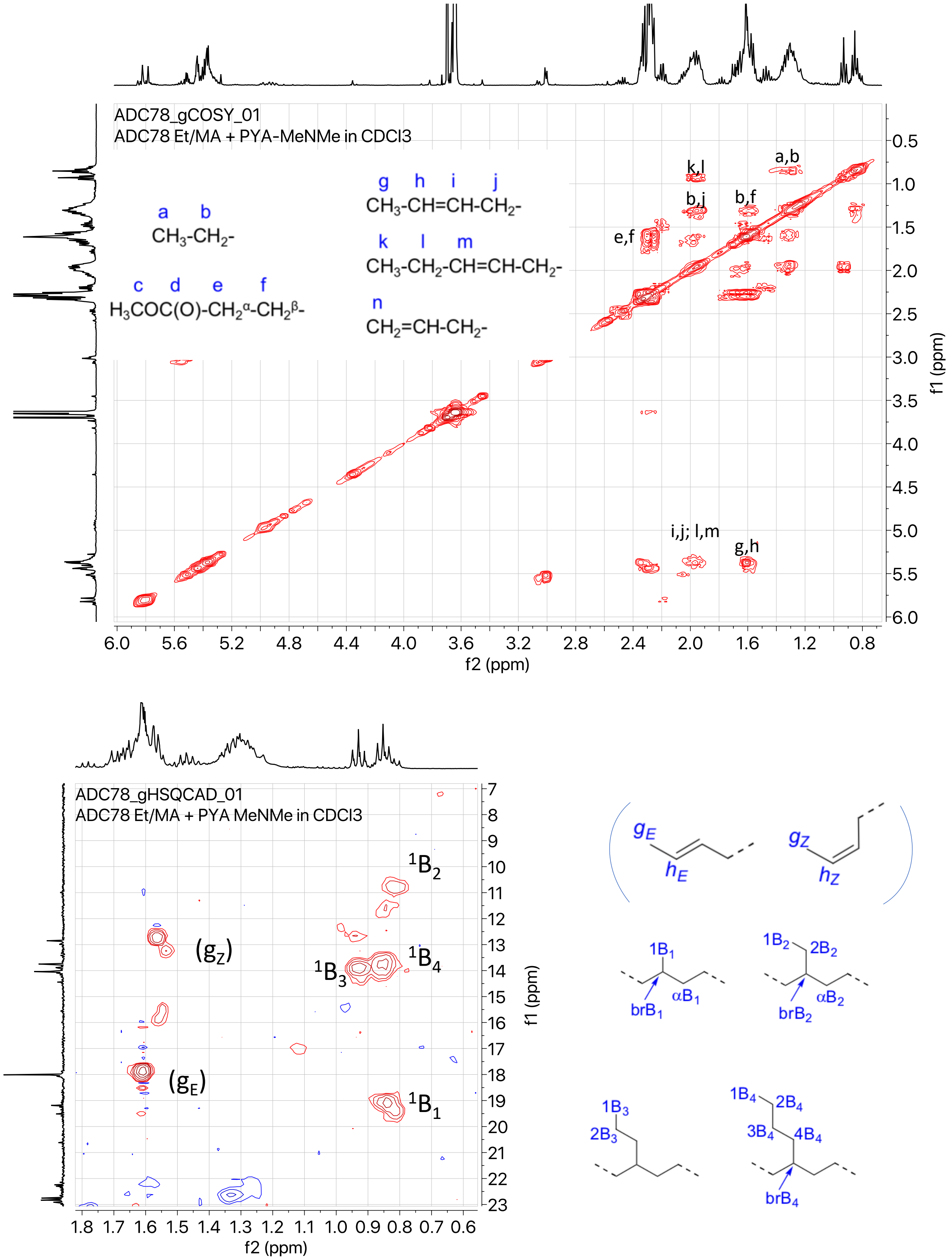

Figure S15. ^{1}H,^{1}H COSY (top) and ^{1}H,^{13}C HSQC (bottom) spectra (CDCl$_3$, 500 MHz, 298 K) of the products obtained from the catalytic run of **10** with MA/ethylene.

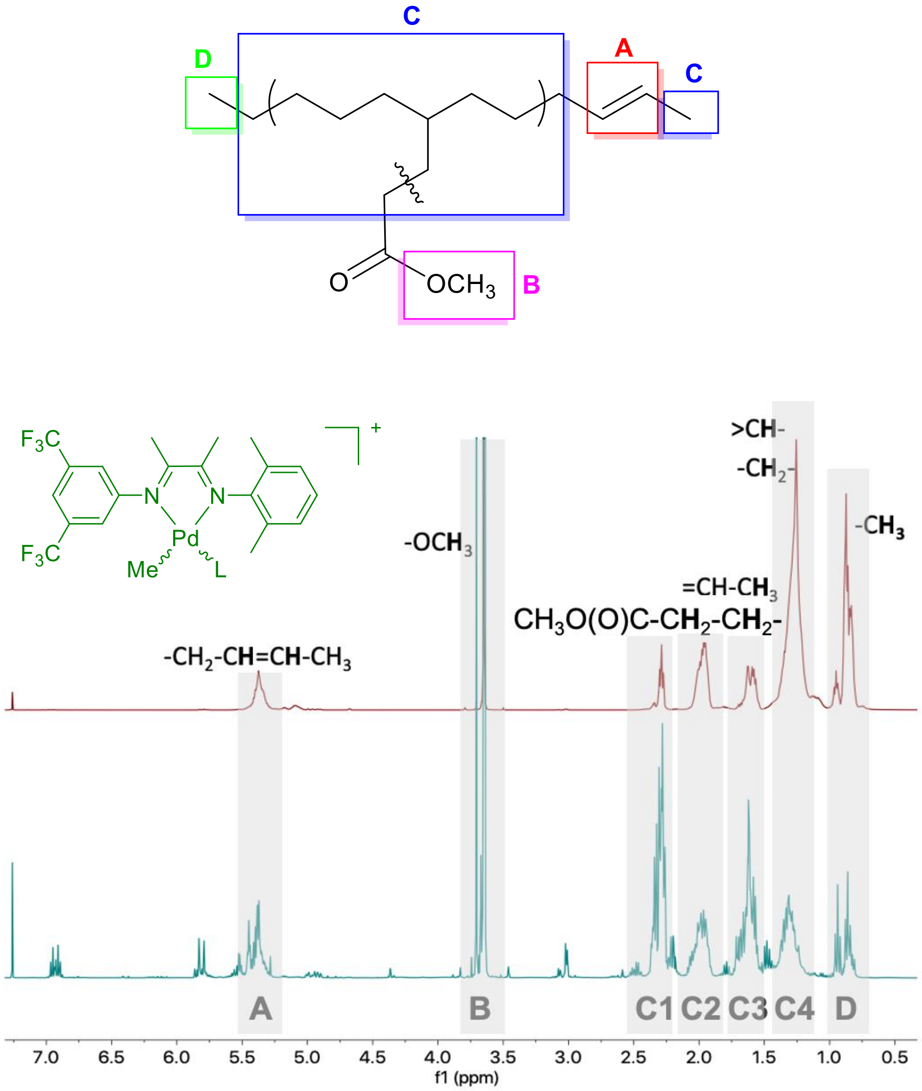

Figure S16. ^{1}H NMR spectra ($CDCl_3$, 400 MHz, 298 K) of: a MA/ethylene copolymer obtained with $[Pd(CH_3)(CH_3CN)(Ar,Ar'\text{-}DAB)][PF_6]$ (top); the catalytic product of a test using **10** (bottom).

Catalytic products were also identified by NMR in comparison with literature.[S1]

[S1] a) S. R. V. Kandula and P. Kumar, *Tetrahedron: Asymmetry*, 2005, **16**, 3268–3274 (α,β- trans pentenoic esters); b) M. Pérez-Venegas, G. Reyes-Rangel, A. Neri, J. Escalante and E. Juaristi, *Beilstein J. Org. Chem.*, 2017, **13**, 1728–1734 (α,β- and β,γ- trans pentenoic, heptanoic esters); c) X. Fang, H. Li, R. Jackstell and M. Beller, *Angew. Chemie - Int. Ed.*, 2014, **53**, 9030–9034 (β,γ- cis and trans pentenoic esters); d) T. Mitsudo, N. Suzuki, T. Kondo and Y. Watanabe, *J. Org. Chem.*, 1994, **59**, 7759–7765; e) M. R. Najafi, M. L. Wang and G. Zweifel, *J. Org. Chem.*, 1991, **56**, 2468–2476 2468 (β,γ- trans heptanoic esters); f) R. Alibés, P. Blanco, E. Casas, M. Closa, P. De March, M. Figueredo, J. Font, E. Sanfeliu and Á. Álvarez-Larena, *J. Org. Chem.*, 2005, **70**, 3157–3167.; g) E. L. Ruggles, P. B. Deker and R. J. Hondal, *Tetrahedron*, 2009, **65**, 1257–1267 (α,β- and β,γ- unsaturated diesters); h) Z.-C. Duan, X.-P. Hu, J. Deng, S.-B. Yu, D.-Y. Wang and Z. Zheng, *Tetrahedron: Asymmetry*, 2009, **20**, 588–592 (branched diesters); i) S. G. Alcock, J. E. Baldwin, R. Bohlmann, L. M. Harwood and J. I. Seeman, *J. Org. Chem.*, 1985, **50**, 3526–3535 (methacrylates)

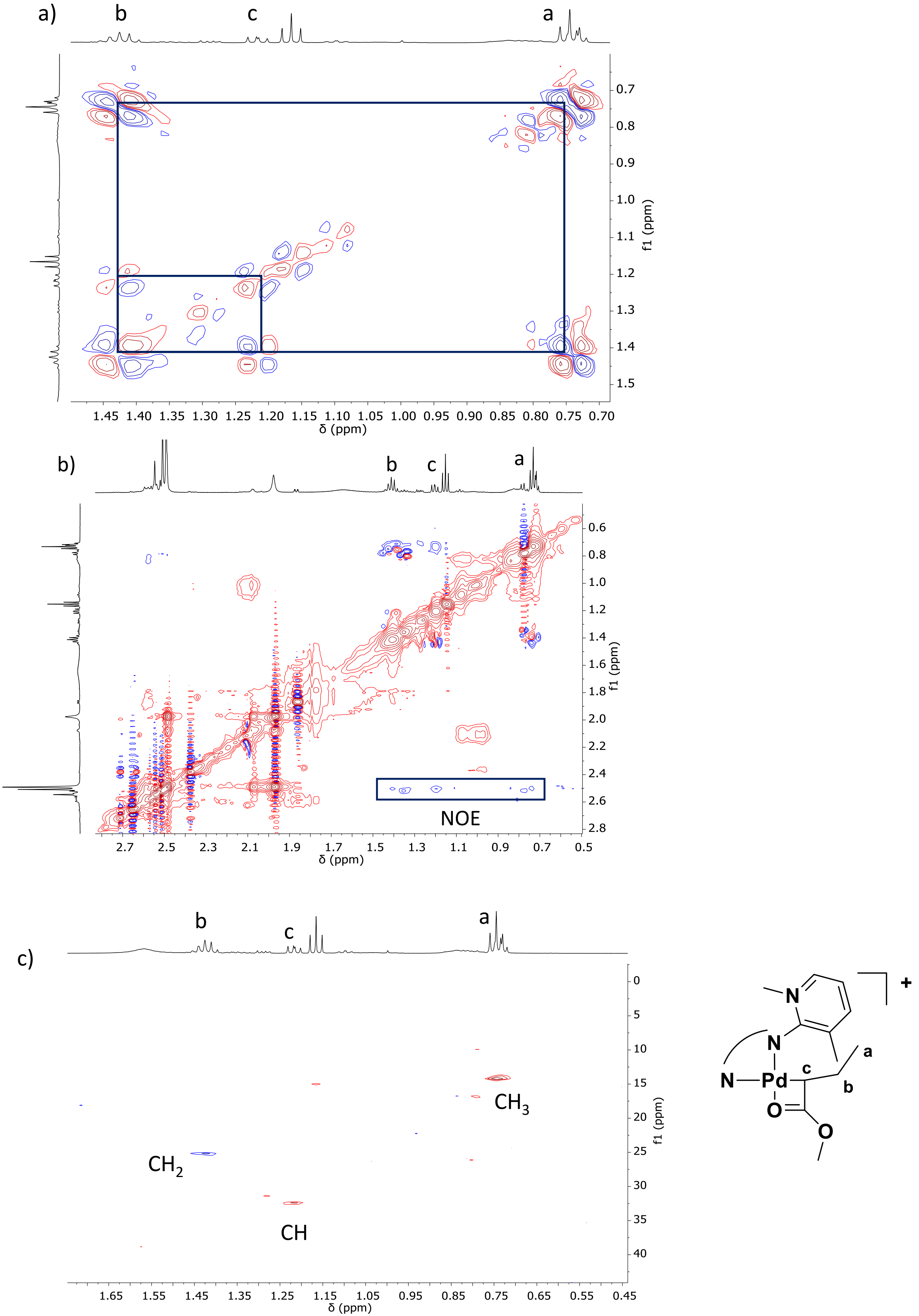

Figure S17. (a) $^1H,^1H$ COSY (b) $^1H,^1H$ NOESY and (c) $^1H,^{13}C$ HSQC spectra of the reactivity of **10** with MA (CD_2Cl_2, 500 MHz, 298 K).

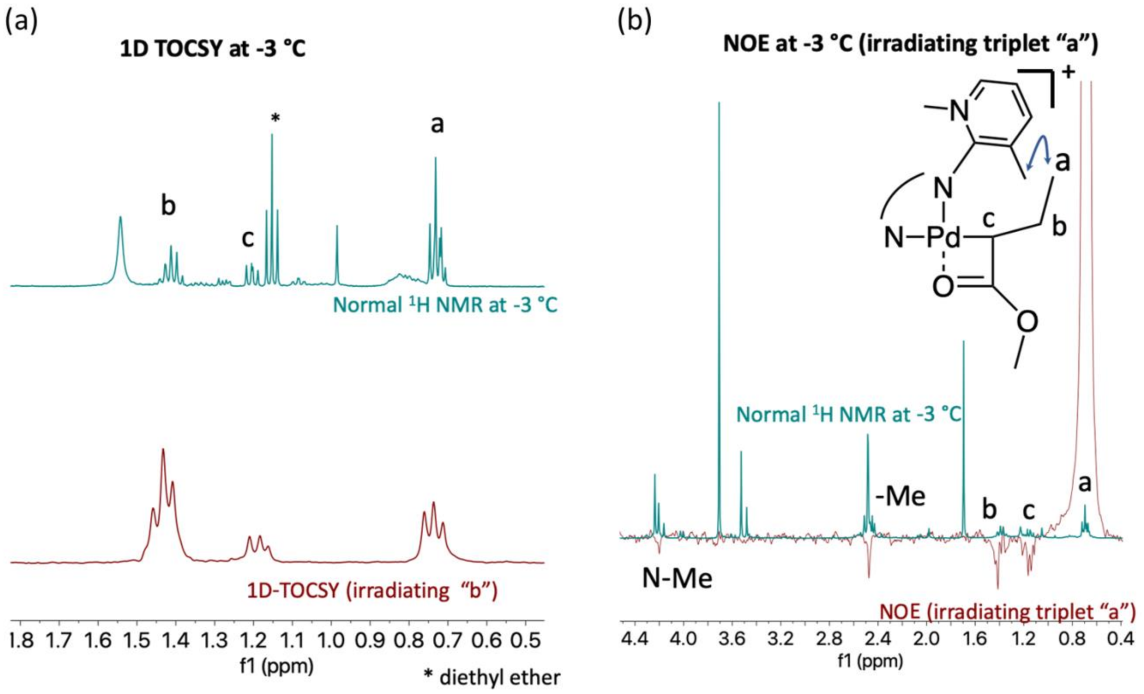

Figure S18. ^{1}H NMR experiments (CD_2Cl_2, 300 MHz, 270 K): (a) 1D Selective TOCSY, (b) 1D Selective NOE (inset: proposed structure).

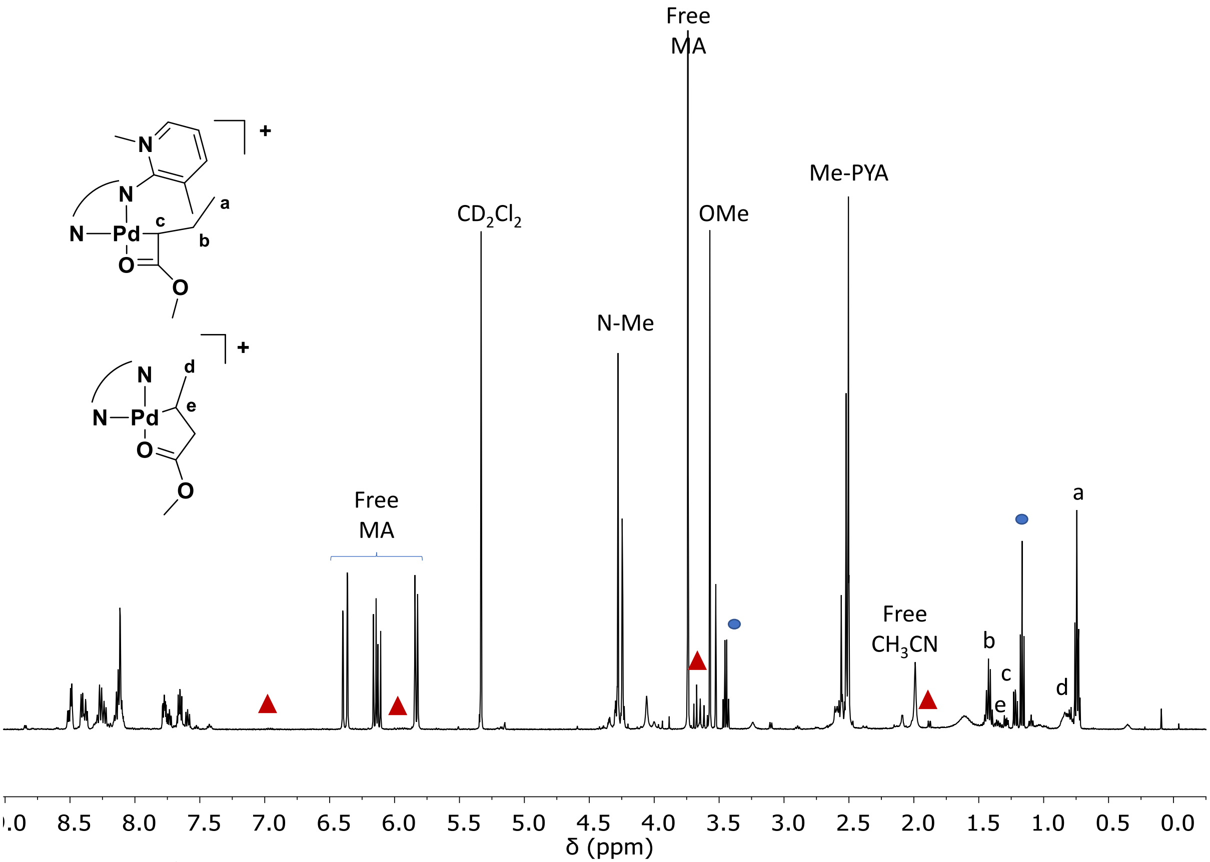

Figure S19. ^{1}H NMR spectrum (CD_2Cl_2, 500 MHz, 298 K) of the reactivity of **10** with MA; ● = diethyl ether, ▲ = methyl crotonate.

Room temperature experiments: Figure S17 (a) shows clear COSY crosspeaks corresponding to an ethyl group – this is further verified from the edited HSQC, where the signal marked “b” has a different phase to the other signals. The interactions are “methyl to methylene to methine” – clearly indicating an A” species. The NOESY (Figure S17b) shows a strong interaction between signals *a* and *b* and a weaker one between signal *a* and a PYA methyl at 2.52 ppm, showing that they are close in space, as we would expect from a Pd-bonded ethyl in the configuration we propose.

Low temperature experiments: The mixture was allowed to react for 2 minutes before being inserted into the NMR machine at 270 K. The initial and final spectra showed little change, indicating that this temperature was sufficient to slow further reaction. The 1D selective TOCSY showed that irradiation at any of the signals *a*, *b* or *c* with a mixing time of 80 ms returned the same spectrum consisting of only *a*, *b* and *c* – indicating that they are all in the same spin system (Figure S18a) - again verifying an ethyl group. A 1D selective NOESY was also attempted (Figure S18b): by irradiating signal *a*, very weak responses are observed to *b* and *c*, as well as to the PYA methyl group and N-Me, verifying the RT 2D-NOESY results supporting the structure as proposed.

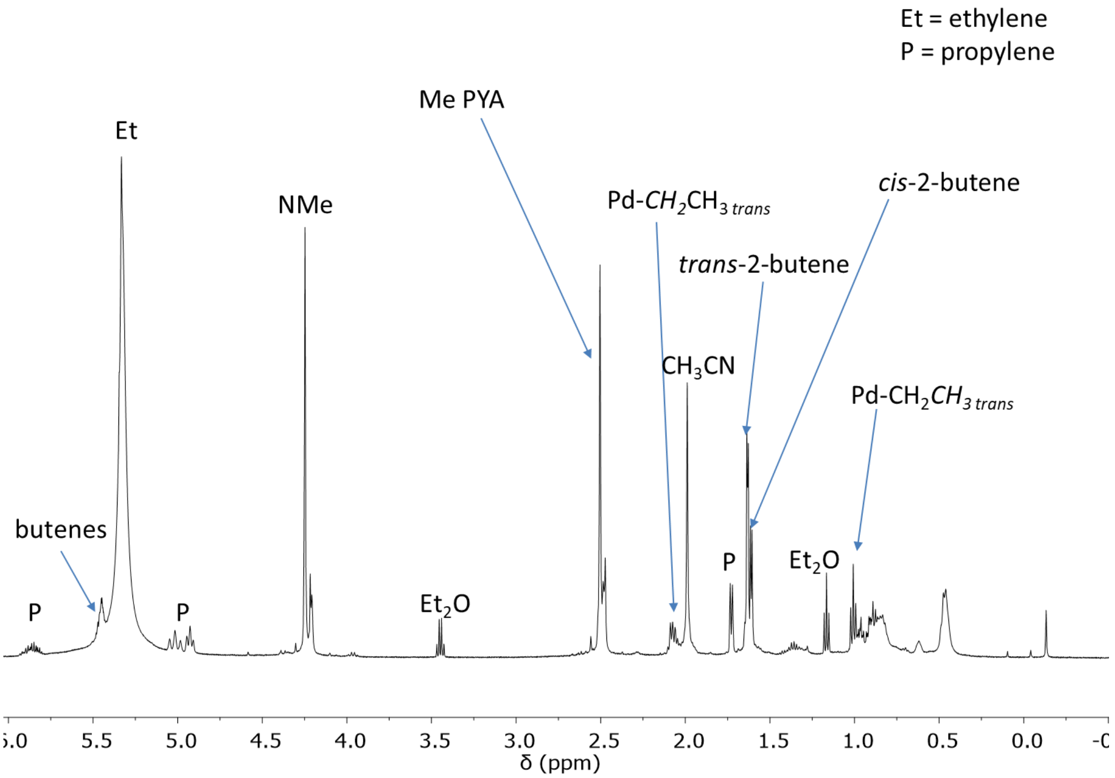

Figure S20. ^{1}H NMR spectrum (CD_2Cl_2, 500 MHz, 298 K) of the reactivity of **10** with ethylene, t = 1 min.

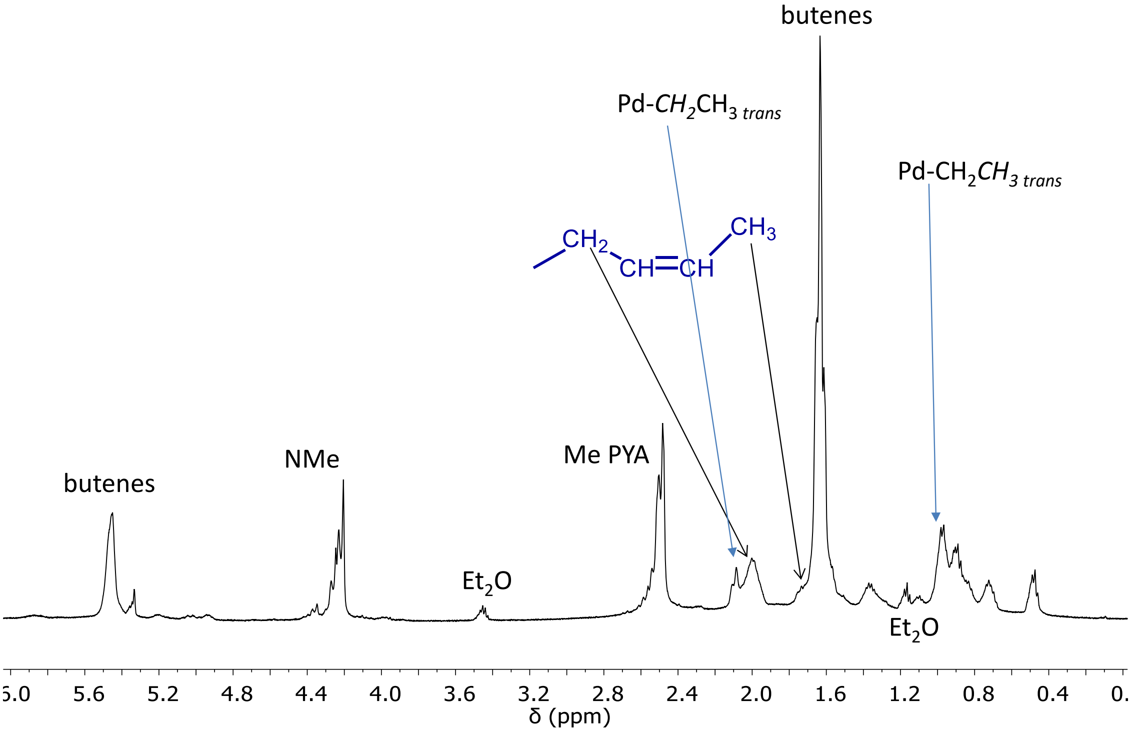

Figure S21. ^{1}H NMR spectrum (CD_2Cl_2, 500 MHz, 298 K) of the reactivity of **10** with ethylene, t = 25 min.

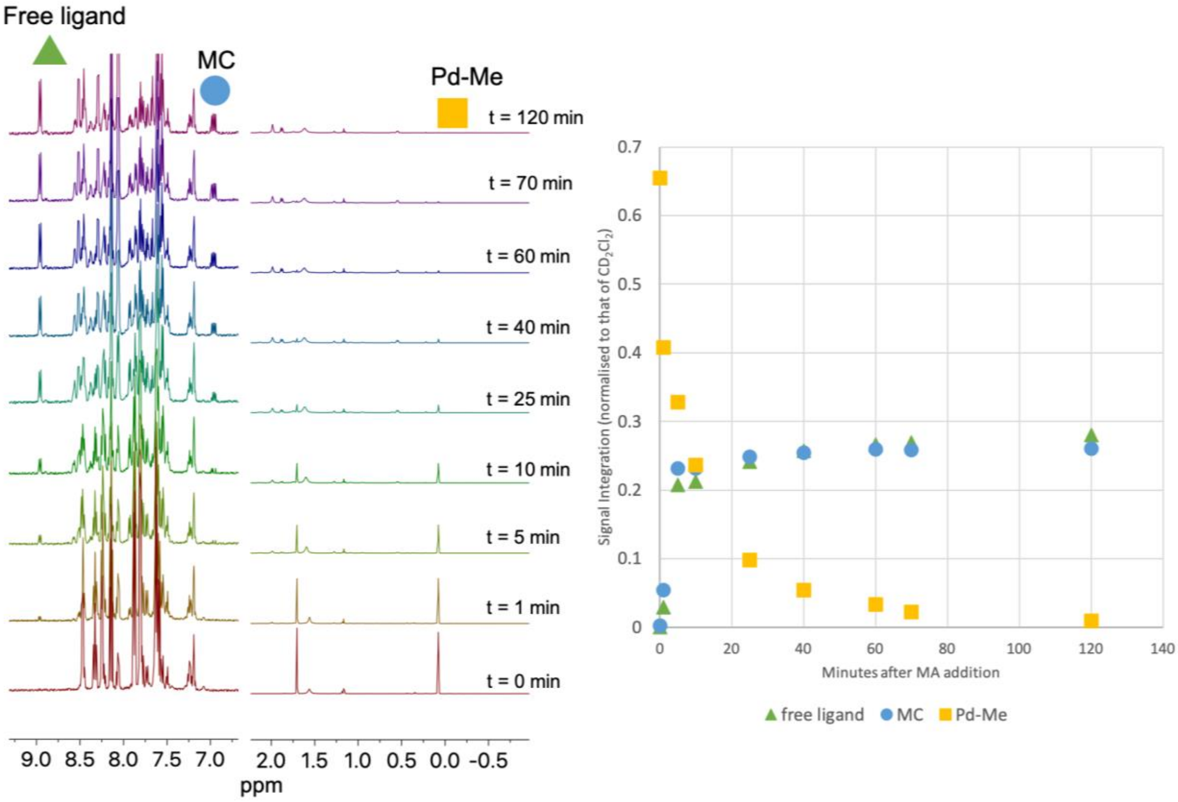

Figure S22. Reactivity tests of **11** with MA: Evolving changes in the ^1H NMR of **11** (CD_2Cl_2, 500 MHz, 298 K). The signals between 6.50 – 9.5 ppm have been made x2.5 more intense. Rough fitting of the trends in the integrals of the signals marked.

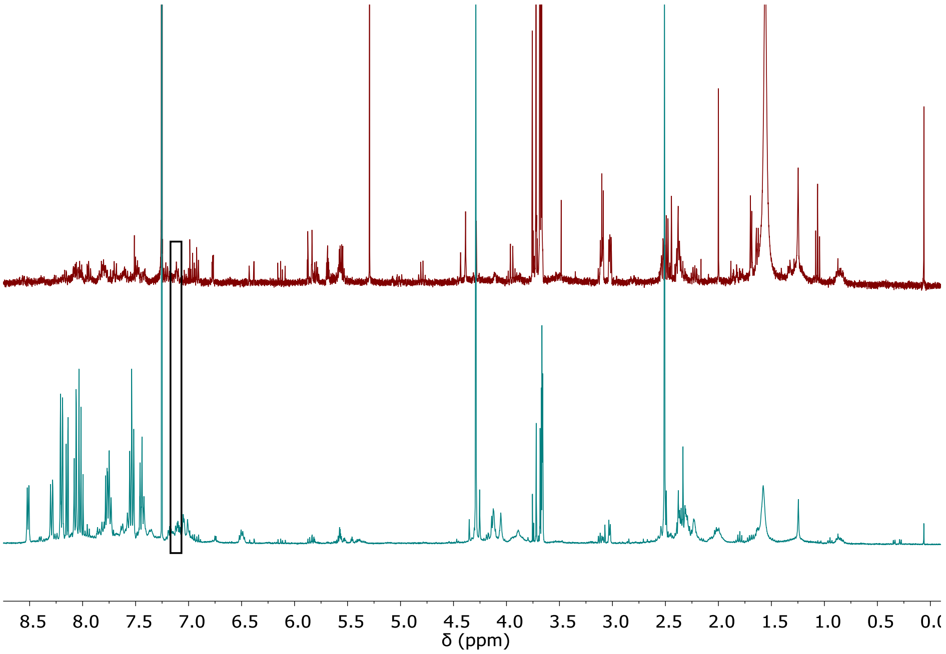

Figure S23. ^1H NMR spectra (CD_2Cl_2, 500 MHz, 298 K) of product of ethylene/MA copolymerization with complex **11** (top) and complex **12** (bottom); black rectangle: signal of complex **13**.

3. Spectroscopic and catalytic properties of 13

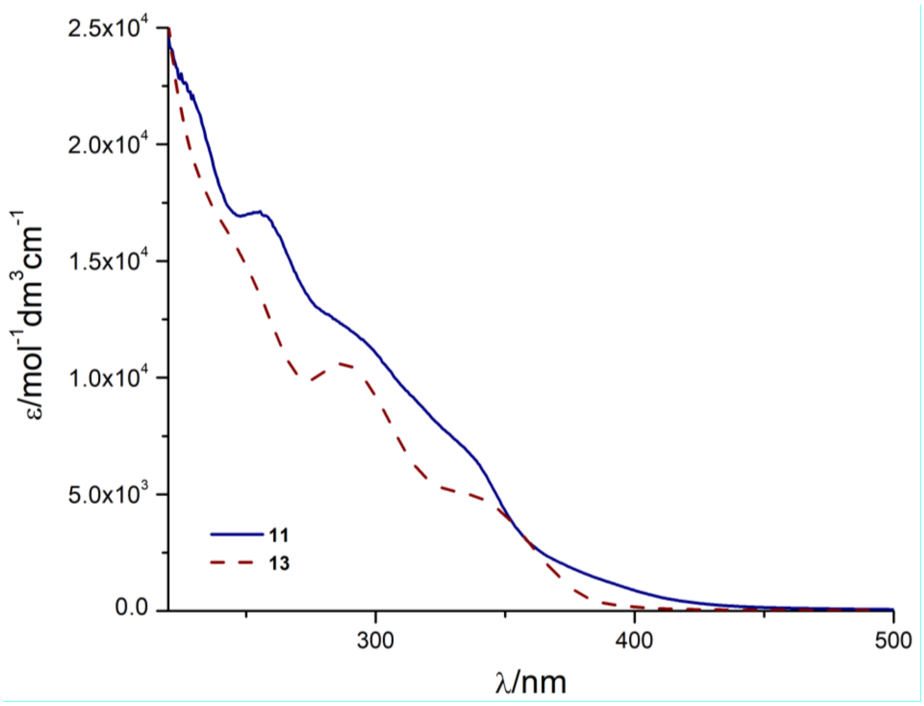

Figure S24. UV-vis spectra of **13** and **11** in acetonitrile.

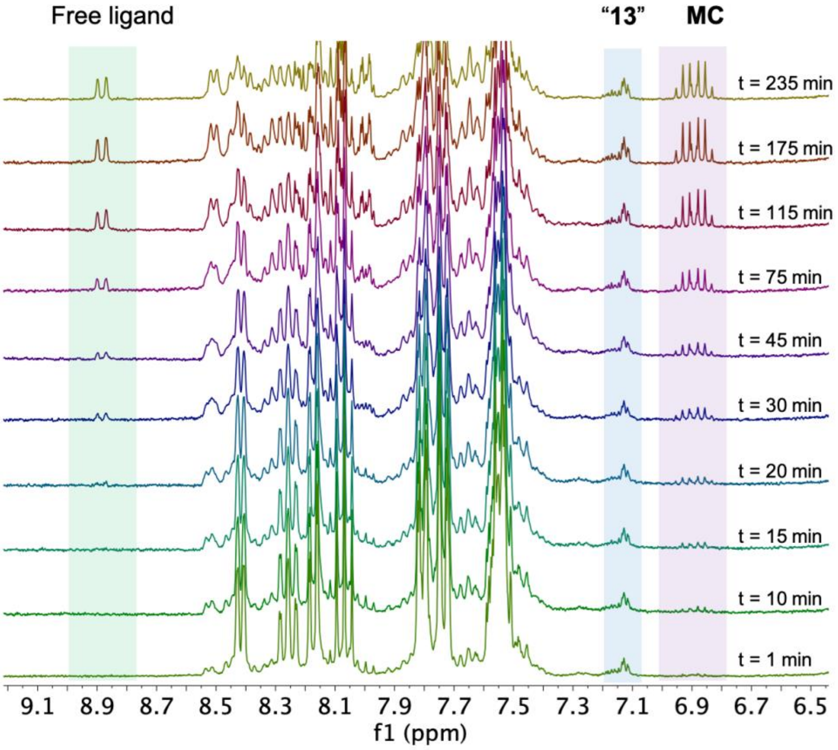

Figure S25. Reactivity test of **11** with MA: Evolving changes in the ^{1}H NMR of **11**, showing the residual cyclometalated **13** remains constant as MC is produced and free ligand is released (CD_2Cl_2, 500 MHz, 298 K).

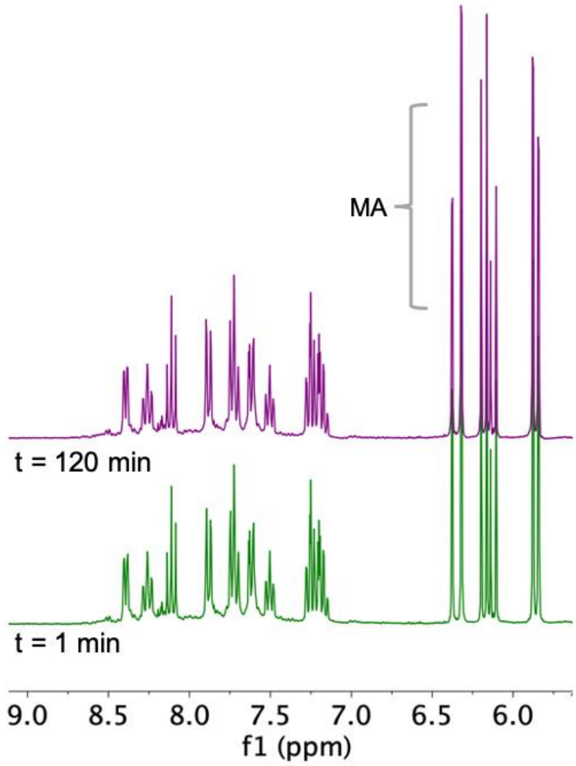

Figure S26. Reactivity test of **13** with MA: comparison of the ^{1}H NMR spectra obtained 1 min (bottom) and 2 h (top) after the addition of methyl acrylate to the sample (CD_3CN, 500 MHz, 298 K), demonstrating no reactivity of MA with complex **13**.

4. Crystallographic details of 13

Details on Structure Determination. A crystal of [$C_{20}H_{17}N_4OPd$][PF_6] was mounted in air at ambient conditions. All measurements were made on a *RIGAKU Synergy S* area-detector diffractometer[S2] using mirror optics monochromated Cu *K*α radiation (λ = 1.54184 Å). The unit cell constants and an orientation matrix for data collection were obtained from a least-squares refinement of the setting angles of reflections in the range 3.8° < θ < 76.4°. A total of 5814 frames were collected using ω scans, with 0.1 and 0.39 seconds exposure time, a rotation angle of 0.5° per frame, a crystal-detector distance of 34.0 mm, at T = 173(2) K.

Data reduction was performed using the *CrysAlisPro*[1] program. The intensities were corrected for Lorentz and polarization effects, and a numerical absorption correction based on gaussian integration over a multifaceted crystal model was applied. Data collection and refinement parameters are given in Table S1.

The structure was solved by direct methods using *SHELXT*,[S3] which revealed the positions of all non-hydrogen atoms of the title compound. The non-hydrogen atoms were refined anisotropically. All H-atoms were placed in geometrically calculated positions and refined using a riding model where each H-atom was assigned a fixed isotropic displacement parameter with a value equal to 1.2Ueq of its parent atom (1.5Ueq for the methyl groups).

Refinement of the structure was carried out on F^2 using full-matrix least-squares procedures, which minimized the function $\Sigma w(F_o^2 - F_c^2)^2$. The weighting scheme was based on counting statistics and included a factor to downweight the intense reflections. All calculations were performed using the *SHELXL-2014/7*[S4] program in OLEX2.[S5] Further crystallographic details are compiled in Table S1 and bond lengths and angles in Tables S2 and S3, respectively. Crystallographic data for the structure of **13** have been deposited with the Cambridge Crystallographic Data Centre (CCDC) as supplementary publication number 2055487.

[S2] Oxford Diffraction (2018). *CrysAlisPro* (Version 1.171.40.37a). Oxford Diffraction Ltd., Yarnton, Oxfordshire, UK.

[S3] G. M. Sheldrick, *Acta Cryst.*, 2015, **A71**, 3-8.

[S4] G. M. Sheldrick, *Acta Cryst.*, 2015, **C71**, 3-8.

[S5] O.V. Dolomanov, L.J. Bourhis, R.J. Gildea, J. A. K. Howard and H. Puschmann, *J. Appl. Cryst.*, 2009, **42**, 339-341.

Table S1. Crystal data and structure refinement for complex 13.

CCDC No.	2055487
Empirical formula	$C_{20}H_{17}F_6N_4OPPd$
Formula weight	580.74
Temperature/K	173.01(10)
Crystal system	triclinic
Space group	P-1
a/Å	7.76590(10)
b/Å	11.65990(10)
c/Å	11.85750(10)
α/°	83.0730(10)
β/°	81.0700(10)
γ/°	85.1350(10)
Volume/$Å^3$	1050.542(19)
Z	2
$\rho_{calc}g/cm^3$	1.836
μ/mm^{-1}	8.543
F(000)	576.0
Crystal size/mm^3	0.21 × 0.072 × 0.042
Radiation	CuKα (λ = 1.54184)
2Θ range for data collection/°	7.592 to 154.33
Index ranges	$-9 \leq h \leq 9$, $-14 \leq k \leq 14$, $-14 \leq l \leq 14$
Reflections collected	20226
Independent reflections	4327 [$R_{int} = 0.0339$, $R_{sigma} = 0.0204$]
Data/restraints/parameters	4327/0/300
Goodness-of-fit on F^2	1.050
Final R indexes [I>=2σ (I)]	$R_1 = 0.0329$, $wR_2 = 0.0822$
Final R indexes [all data]	$R_1 = 0.0332$, $wR_2 = 0.0824$
Largest diff. peak/hole / e $Å^{-3}$	1.28/–0.84

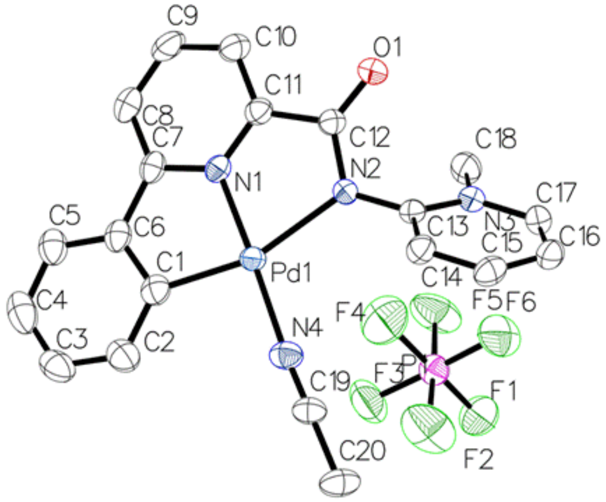

Figure S27. ORTEP of complex **13** (50% probability thermal ellipsoids, H-atoms omitted for clarity).

Table S2. Bond lengths for complex 13.

Atom	Atom	Length/Å	Atom	Atom	Length/Å
Pd^{1}	N^{1}	1.959(2)	C^{5}	C^{6}	1.393(5)
Pd^{1}	C^{1}	2.010(3)	C^{6}	C^{7}	1.470(5)
Pd^{1}	N^{2}	2.146(2)	C^{7}	C^{8}	1.385(5)
Pd^{1}	N^{4}	2.005(3)	C^{8}	C^{9}	1.375(5)
O^{1}	C^{12}	1.227(4)	C^{9}	C^{10}	1.387(5)
N^{1}	C^{7}	1.354(4)	C^{10}	C^{11}	1.379(4)
N^{1}	C^{11}	1.337(4)	C^{11}	C^{12}	1.507(4)
C^{1}	C^{2}	1.385(5)	C^{13}	C^{14}	1.398(4)
C^{1}	C^{6}	1.409(5)	C^{14}	C^{15}	1.371(5)
N^{2}	C^{12}	1.362(4)	C^{15}	C^{16}	1.387(5)
N^{2}	C^{13}	1.375(4)	C^{16}	C^{17}	1.353(5)
C^{2}	C^{3}	1.376(6)	C^{19}	C^{20}	1.459(5)
N^{3}	C^{13}	1.361(4)	P^{1}	F^{1}	1.563(3)
N^{3}	C^{17}	1.367(4)	P^{1}	F^{2}	1.579(3)
N^{3}	C^{18}	1.470(4)	P^{1}	F^{3}	1.594(3)
C^{3}	C^{4}	1.403(6)	P^{1}	F^{4}	1.587(3)
N^{4}	C^{19}	1.133(4)	P^{1}	F^{5}	1.583(3)
C^{4}	C^{5}	1.396(6)	P^{1}	F^{6}	1.573(3)

Table S3. Bond Angles for Complex 13.

Atom	Atom	Atom	Angle/°	Atom	Atom	Atom	Angle/°
N^1	Pd^1	C^1	81.11(12)	C^{11}	C^{10}	C^9	118.2(3)
N^1	Pd^1	N^2	79.04(10)	N^1	C^{11}	C^{10}	120.5(3)
N^1	Pd^1	N^4	177.47(11)	N^1	C^{11}	C^{12}	115.6(3)
C^1	Pd^1	N^2	160.04(12)	C^{10}	C^{11}	C^{12}	124.0(3)
N^4	Pd^1	C^1	96.56(13)	O^1	C^{12}	N^2	126.7(3)
N^4	Pd^1	N^2	103.26(11)	O^1	C^{12}	C^{11}	120.4(3)
C^7	N^1	Pd^1	118.5(2)	N^2	C^{12}	C^{11}	112.9(3)
C^{11}	N^1	Pd^1	118.9(2)	N^2	C^{13}	C^{14}	120.6(3)
C^{11}	N^1	C^7	122.6(3)	N^3	C^{13}	N^2	121.1(3)
C^2	C^1	Pd^1	129.2(3)	N^3	C^{13}	C^{14}	118.2(3)
C^2	C^1	C^6	117.9(3)	C^{15}	C^{14}	C^{13}	121.1(3)
C^6	C^1	Pd^1	112.9(2)	C^{14}	C^{15}	C^{16}	119.3(3)
C^{12}	N^2	Pd^1	112.98(19)	C^{17}	C^{16}	C^{15}	119.0(3)
C^{12}	N^2	C^{13}	119.7(2)	C^{16}	C^{17}	N^3	122.0(3)
C^{13}	N^2	Pd^1	127.11(19)	N^4	C^{19}	C^{20}	178.7(4)
C^3	C^2	C^1	120.4(4)	F^1	P^1	F^2	91.7(2)
C^{13}	N^3	C^{17}	120.4(3)	F^1	P^1	F^3	88.94(18)
C^{13}	N^3	C^{18}	121.9(3)	F^1	P^1	F^4	175.9(2)
C^{17}	N^3	C^{18}	117.6(3)	F^1	P^1	F^5	89.5(2)
C^2	C^3	C^4	121.7(4)	F^1	P^1	F^6	92.13(19)
C^{19}	N^4	Pd^1	173.5(3)	F^2	P^1	F^3	88.20(17)
C^5	C^4	C^3	119.0(4)	F^2	P^1	F^4	91.3(2)
C^6	C^5	C^4	118.6(4)	F^2	P^1	F^5	177.21(19)
C^1	C^6	C^7	115.0(3)	F^4	P^1	F^3	88.48(19)
C^5	C^6	C^1	122.4(3)	F^5	P^1	F^3	89.32(15)
C^5	C^6	C^7	122.6(3)	F^5	P^1	F^4	87.4(2)
N^1	C^7	C^6	112.3(3)	F^6	P^1	F^2	93.02(17)
N^1	C^7	C^8	118.6(3)	F^6	P^1	F^3	178.36(17)
C^8	C^7	C^6	129.1(3)	F^6	P^1	F^4	90.39(19)
C^9	C^8	C^7	119.7(3)	F^6	P^1	F^5	89.44(16)
C^8	C^9	C^{10}	120.5(3)				